República de Colombia
Ministerio de Educación Nacional

La Universidad Nacional de Colombia

Teniendo en cuenta que

Franklin Alexander Paz Triviño

C.C. 98.704.990 de Bello

cumplió satisfactoriamente todos los requisitos académicos reglamentarios del Plan de Estudios de Posgrado, le confiere el Título de

Magíster en Ingeniería Mecánica

En la ciudad de Medellín, a los 07 días del mes de abril de 2017

Decanatura de Facultad | Rectoría | Secretaría General

Registro n.° 2733, Folio 83 del Libro de Diplomas n.° 2
de la Sede Medellín, Facultad de Minas

48395
THOMAS GREG & SONS.

1803

LA UNIVERSIDAD DE ANTIOQUIA

PERSONERÍA JURÍDICA LEY 71 DE 1878 DEL ESTADO SOBERANO DE ANTIOQUIA Y LEY 153 DE 1887

EN ATENCIÓN A QUE

FRANKLIN ALEXÁNDER PAZ TRIVIÑO

IDENTIFICADO CON CÉDULA DE CIUDADANÍA 98704990

HA COMPLETADO TODOS LOS REQUISITOS QUE LOS ESTATUTOS UNIVERSITARIOS EXIGEN PARA OPTAR AL TÍTULO DE

INGENIERO MECÁNICO

LE EXPIDE EL PRESENTE DIPLOMA, EN TESTIMONIO DE ELLO, SE FIRMA EN MEDELLÍN REPÚBLICA DE COLOMBIA, EL 19 DE SEPTIEMBRE DE 2008

ALBERTO URIBE CORREA
RECTOR

ANA LUCÍA HERRERA GÓMEZ
SECRETARIA

ELKIN LIBARDO RÍOS ORTIZ
DECANO

42711

THOMAS GREG & SONS.

Universidad Pontificia Bolivariana

Medellín, 23 de junio de 2020

EL JEFE DE
FORMACIÓN CONTINUA

HACE CONSTAR QUE:

El señor **Franklin Alexander Paz Triviño**, identificado con Cédula de Ciudadanía 98.704.990, se encuentra participando de la diplomatura **"La docencia universitaria: pedagogía, currículo y didácticas"** que se realiza del 10 de marzo al 30 de julio de 2020, con una intensidad de 123 horas, de las cuales faltan por cursar 57 horas.

Esta constancia se expide a solicitud del interesado.



JUAN CARLOS PÉREZ PÉREZ
Katherine C

Libertad y orden
REPÚBLICA DE COLOMBIA

El Servicio Nacional de Aprendizaje SENA

En cumplimiento de la Ley 119 de 1994

Hace constar que

FRANKLIN ALEXANDER PAZ TRIVINO

Con Cédula de Ciudadanía No. 98.704.990

Cursó y aprobó la acción de Formación

GESTION DE PROYECTOS EN MICROSOFT PROJECT

con una duración de 40 horas

En testimonio de lo anterior, se firma el presente en Medellín, a los catorce (14) días del mes de mayo de dos mil diez (2010)

Firmado Digitalmente por
NOHORA JUDITH HERNANDEZ LOPEZ
SERVICIO NACIONAL DE APRENDIZAJE SENA
Autenticidad del Documento
Bogotá - Colombia

NOHORA JUDITH HERNANDEZ LOPEZ
SUBDIRECTOR
CENTRO PARA EL DESARROLLO DEL HABITAT Y LA CONSTRUCCIÓN
REGIONAL ANTIOQUIA

1145179 - 14/05/2010
FECHA REGISTRO

La autenticidad de este documento puede ser verificada en el registro electrónico que se encuentra en la página web http://certificados.sena.edu.co, bajo el número 92030056218CC98704990C.

INTERNATIONAL ENGLISH LANGUAGE TESTING SYSTEM

Test Report Form

ACADEMIC

NOTE *Admission to undergraduate and post graduate courses should be based on the ACADEMIC Reading and Writing Modules. GENERAL TRAINING Reading and Writing Modules are* ***not*** *designed to test the full range of language skills required for academic purposes. It is recommended that the candidate's language ability as indicated in this Test Report Form be re-assessed* ***after two years*** *from the date of the test.*

Centre Number: CO001 | Date: 20/SEP/2014 | Candidate Number: 003946

Candidate Details

Family Name: PAZ TRIVIÑO

First Name: FRANKLIN ALEXANDER

Candidate ID: 98704990



Date of Birth: 15/04/1983 | Sex (M/F): M | Scheme Code: Private Candidate

Country or Region of Origin:

Country of Nationality: COLOMBIA

First Language: SPANISH

Test Results

Listening	Reading	Writing	Speaking	Overall Band Score
5.0	5.5	5.5	5.5	5.5

Administrator Comments

Centre stamp

BRITISH COUNCIL Colombia

Validation stamp

IELTS

Administrator's Signature

Date: 02/10/2014

Test Report Form Number: 14CO003946PAZF001A

BRITISH COUNCIL

idp IELTS AUSTRALIA

CAMBRIDGE ENGLISH Language Assessment
Part of the University of Cambridge

The validity of this IELTS Test Report Form can be verified online by recognising organisations at http://ielts.ucles.org.uk

END/NDT
Ensayos No Destructivos S.A.S.

CERTIFICA QUE:

FRANKLIN ALEXANDER PAZ TRIVIÑO

CC 98.704.990

Reunió los requisitos del Procedimiento de Calificación y Certificación de Personal en Ensayos no Destructivos de END/NDT ENSAYOS NO DESTRUCTIVOS S.A.S. que es basado en la SNT-TC-1A – 2011 de la ASNT, por lo tanto se califica como:

NIVEL II EN RADIOGRAFIA INDUSTRIAL

EXAMEN	REQUERIDO	REAL
GENERAL	70 % Mín.	**83 %**
ESPECÍFICO	70 % Mín.	**77 %**
PRÁCTICO	70 % Mín.	**90 %**
TOTAL	80% Mín.	**83 %**

Certificado Número: 1085

Fecha Entrenamiento: 21 al 30 de Noviembre de 2015. Duración: 80 horas.

Fecha de Certificación: 05 de Diciembre de 2015
Fecha de Vencimiento Certificación: 04 de Diciembre de 2020

Esta calificación permanecerá vigente siempre y cuando el Inspector antes mencionado cumpla con los requisitos establecidos en el Procedimiento de Calificación y Certificación de END/NDT ENSAYOS NO DESTRUCTIVOS S.A.S., la práctica escrita del empleador, los códigos, normas y otros documentos que aplique.

Rionegro, Colombia, 05 de Diciembre de 2015

END/NDT ENSAYOS NO DESTRUCTIVOS S.A.S.
AGENCIA EXTERNA / SERVICIOS END/NDT NIVEL III
TLF: (57) 3108211495, http://endndt.wix.com/endndt
endndt@hotmail.com, evm689@hotmail.com

PEDRO R. BEJARANO C
ASNT LEVEL III
ID 163759

ING. PEDRO RICARDO BEJARANO C.
NDT LEVEL III – ASNT ID 163759

ACOSEND

ASOCIACIÓN COLOMBIANA DE SOLDADURA Y ENSAYOS NO DESTRUCTIVOS

ICNDT

Miembros del Comite Internacional de Ensayos No Destructivos

Hace Constar

Que **FRANKLIN ALEXANDER PAZ TRIVIÑO**

Participó en "SEMINARIO DE ACTUALIZACION EN CONSTRUCCIONES SOLDADAS"

Duración 40 HORAS

Asociación Colombiana de Soldadura y Ensayos No Destructivos

ACOSEND

Lugar y Fecha Bogotá, 25 de Junio de 2010

Registro ACS - 1860

HOBART INSTITUTE OF WELDING TECHNOLOGY

presents this certificate to

Franklin Paz

for the successful completion of

Visual Inspection

C.E.U. 1.4

September 21, 2012



en3TIjUd8V

Ron L. Scott, Vice President/General Manager

Elmer R. Swank Jr., Supervisor of Technical Training

West Arco

Número UNO en soldadura

SOLDADURAS ESPECIALES

West Rode

TECNOLOGIA A SU SERVICIO

El Instituto de Soldadura West Arco

Certifica que:

FRANKLIN PAZ TRIVIÑO

C.C. 98.704.990

El Señor(a): _____

Asistió al: **CURSO DE INSPECCION VISUAL Y DEFECTOS EN SOLDADURA**

Ciudad y Fecha: YOPAL, 29 Y 30 DE JUNIO DE 2010

INTENSIDAD: 16 HORAS

Coordinador Comercial

Coordinador Técnico

WEST ARCO
INSTITUTO DE SOLDADURA

CERTIFICA QUÉ:

FRANKLIN ALEXANDER PAZ TRIVIÑO

EL SEÑOR (A): C.C. 98.704.990 DE BELLO

ASISTIO AL

CURSO DE SUPERVISIÓN EN SOLDADURAS DE PRODUCCION

INTENSIDAD: **INTENSIDAD 24 HORAS**

CIUDAD Y FECHA: BOGOTA D.C., 7, 8 Y 9 DE JULIO DE 2010

JEFE INSTITUTO DE SOLDADURA

SOLDADURAS WEST ARCO
SOLUCIÓN INTEGRAL EN UNIÓN Y CORTE DE MATERIALES

West arco
Número UNO en soldadura

REGIONAL ANTIOQUIA

EL CENTRO DE TECNOLOGÍA DE LA MANUFACTURA AVANZADA.

CERTIFICA

Que FRANKLIN ALEXANDER PAZ TRIVINO identificado(a) con Cédula de Ciudadanía No 98.704.990 de , realizó y aprobó el curso de BASICO EN REPARACION DE MOTORES DIESEL con una intensidad horaria de Ochenta (80) y obtuvo una evaluación Apto (A) con una equivalencia de (4.5).

Equivalencia de Evaluaciones:
D: Reprobo
A: Aprobo

Se expide en Medellín, a los trece (13) días del mes de julio de dos mil diez (2010)

Firmado Digitalmente por
GUSTAVO ADOLFO LOPEZ DE MESA GUTIERREZ
SERVICIO NACIONAL DE APRENDIZAJE SENA
Autenticidad del Documento
Bogotá - Colombia

GUSTAVO LOPEZ DE MESA GUTIERREZ
SUBDIRECTOR CENTRO DE TECNOLOGÍA DE LA MANUFACTURA AVANZADA.
REGIONAL ANTIOQUIA

La autenticidad de este documento puede ser verificada en el registro electrónico que se encuentra en la página web http://certificados.sena.edu.co, bajo el número 92040055297CC98704990E.

TOEFL iBT® Test Taker Score Report

THIS IS A PDF DOWNLOADED AND PRINTED BY THE TEST TAKER, INTENDED FOR THE TEST TAKER'S PERSONAL RECORDS.



Name: Paz Trivino, Franklin Alexander
Last (Family/Surname) Name, First (Given) Name Middle Name

Email: franklinpaz1025@gmail.com

Gender: M

Registration Number: 0000 0000 3394 0407

Date of Birth: 15 Apr 1983

Test Date: 25 Aug 2018 **Sponsor Code:**

Paz Trivino, Franklin Alexander
Circular 73A # 39-58
Medellin, Colombia 050018
Colombia

Country of Birth: Colombia

Native Language: SPANISH

Test Center: STN15390A - Universidad Catolica de Oriente

Test Center Country: Colombia

Inst. Code | **Dept. Code**

TOEFL iBT Scaled Scores

Reading	17
Listening	18
Speaking	20
Writing	18
Total Score	**73**

19

Security Identification

ID Type: Passport **ID No.:** xxxxxxxxxxxxxxxxxxxx7066 **Issuing Country:** Colombia

Reading Skills	Level	Your Performance
Reading	Intermediate	Test takers who receive a score at the **INTERMEDIATE** level, as you did, typically understand academic texts in English that require a wide range of reading abilities, although their understanding of certain parts of the texts is limited. Test takers who receive a score at the **INTERMEDIATE** level typically • have a good command of common academic vocabulary but still have some difficulty with high-level vocabulary; • have a very good understanding of grammatical structure; • can understand and connect information, make appropriate inferences, and synthesize information in a range of texts but have more difficulty when the vocabulary is high level and the text is conceptually dense; • can recognize the expository organization of a text and the role that specific information serves within a larger text but have some difficulty when these are not explicit or easy to infer from the text; and • can abstract major ideas from a text but have more difficulty doing so when the text is conceptually dense.

Listening Skills	Level	Your Performance
Listening	Intermediate	Test takers who receive a score at the **INTERMEDIATE** level, as you did, typically understand conversations and lectures in English that present a wide range of listening demands. These demands can include difficult vocabulary (uncommon terms or colloquial or figurative language), complex grammatical structures, and/or abstract or complex ideas. However, lectures and conversations that require the listener to make sense of unexpected or seemingly contradictory information may present some difficulty. When listening to conversations and lectures like these, test takers at the **INTERMEDIATE** level typically can • understand explicitly stated main ideas and important details, especially if they are reinforced, but may have difficulty understanding main ideas that must be inferred or important details that are not reinforced; • understand how information is being used (for example, to provide support or describe a step in a complex process); • recognize how pieces of information are connected (for example, in a cause-and-effect relationship); • understand, though perhaps not consistently, ways that speakers use language for purposes other than to give information (for example, to emphasize a point, express agreement or disagreement, or convey intentions indirectly); and • synthesize information from adjacent parts of a lecture or conversation and make correct inferences on the basis of that information, but may have difficulty synthesizing information from separate parts of a lecture or conversation.

THIS IS A TEST TAKER COPY OF THE TOEFL SCORE REPORT

Copyright © 2015 by Educational Testing Service. All rights reserved. ETS, the ETS logos, TOEFL, and TOEFL iBT are registered trademarks of Educational Testing Service (ETS) in the United States and other countries.

Speaking Skills	Level*	Your Performance
Speaking about Familiar Topics	Good	Your responses indicate an ability to communicate your personal experiences and opinions effectively in English. Overall, your speech is clear and fluent. Your use of vocabulary and grammar is effective with only minor errors. Your ideas are generally well developed and expressed coherently.
Speaking about Campus Situation	Fair	Your responses demonstrate an ability to speak in English about reading material and experiences typically encountered by university students. You are able to convey relevant information about conversations, newspaper articles, and campus bulletins; however, some details are missing or inaccurate. Limitations of grammar, vocabulary, and pronunciation at times cause difficulty for the listener. However, they do not seriously interfere with overall communication.
Speaking about Academic Course Content	Limited	In your responses, you are able to use English to talk about the basic ideas from academic reading or lecture materials, but, in general, you include few relevant or accurate details. It is sometimes difficult for listeners to understand your responses because of problems with grammar, vocabulary, and pronunciation. Overall, you are able to respond in a general way to the questions, but the amount of information in your responses is limited and the expression of ideas is often vague and unclear.
Writing Skills	**Level***	**Your Performance**
Writing based on Reading and Listening	Fair	You responded to the task, relating the lecture to the reading, but your response indicates weaknesses such as • an important idea or ideas may be missing, unclear, or inaccurate; • there may be unclarity in how the lecture and the reading passage are related; and/or • grammatical mistakes or vague/incorrect uses of words may make the writing difficult to understand.
Writing based on Knowledge and Experience	Fair	You expressed ideas with reasons, examples, and details, but your response indicated weaknesses such as • you may not provide enough specific support and development for your main points; • your ideas may be difficult to follow because of how you organize your essay or because of the language you use to connect your ideas; and/or • grammatical mistakes or vague/incorrect uses of words may make the writing difficult to understand.

THIS IS A PDF DOWNLOADED AND PRINTED BY THE TEST TAKER, INTENDED FOR THE TEST TAKER'S PERSONAL RECORDS.

This score report provides four section scores and a total score. An analysis of your strengths and weaknesses in English is included. The level pertaining to each skill should not be generalized beyond the performance on this test. Skill levels and their associated descriptions are not intended for use by institutions as part of their admissions criteria and will not be shared unless you grant permission.

Information About Scores: The following scaled scores are reported for the TOEFL iBT test. A total score is not reported when one or more sections have not been administered. These scores have the following ranges:

Sections	Scaled Scores
Reading	0-30
Listening	0-30
Speaking	0-30
Writing	0-30
Total Score	0-120

Score Legends:

Reading Skills	
Level	**Total Scaled Score Range**
High	22-30
Intermediate	15-21
Low	0-14

Speaking Skills	
Level	**Total Scaled Score Range**
Good	26-30
Fair	18-25
Limited	10-17
Weak	0-9

Listening Skills	
Level	**Total Scaled Score Range**
High	22-30
Intermediate	14-21
Low	0-13

Writing Skills	
Level	**Total Scaled Score Range**
Good	24-30
Fair	17-23
Limited	1-16
Score of Zero	0

Institution Codes: The code numbers shown on page 1 of this report are the ones you selected before you took the test. If any institution code you selected is missing, it was incorrect and the TOEFL® Program was unable to send a score report to that institution.

DEPT.	WHERE THE REPORT WAS SENT
00	Admissions office for undergraduate study or an institution or agency that is not a college or university
01, 04-99	Admissions office for graduate study in a field other than management (business) or law according to the codes selected when you registered
02	Admissions office of a graduate school of management (business)
03	Admissions office of a graduate school of law

Additional information about TOEFL iBT scores can be found on the Test Takers section of the TOEFL website at **www.ets.org/toefl.**

* Skill levels for speaking and writing individual skills are estimates of performance at the *item* level. The total writing and speaking scaled scores and ranges are more accurate. Therefore it is not appropriate to combine the individual skill levels. Doing so may lead to apparent inconsistencies between the diagnostic feedback and reported writing and speaking scores.

IMPORTANT NOTE TO SCORE USERS: This PDF score report was downloaded and printed by the test taker. It is not an Official Score Report sent by ETS directly to an organization designated by the test taker. If you find it necessary to verify the scores on this report, please contact the TOEFL Score Verification Service at +1-800-257-9547 or +1-609-771-7100. Scores more than two years old cannot be reported or validated.

THIS IS TEST TAKER COPY OF THE TOEFL SCORE REPORT

UNIVERSIDAD NACIONAL DE COLOMBIA
SEDE MEDELLÍN
FACULTAD DE MINAS



DYNA
http://dyna.medellin.unal.edu.co/

Wear resistance and hardness of nanostructured hardfacing coatings

Franklin Paz-Triviño [a], Robison Buitrago-Sierra[b] & Juan Felipe Santa-Marín [a, b]

[a] *Tribology and Surfaces Group, Universidad Nacional de Colombia, Medellín, Colombia. franklinpaz1025@gmail.com, jfsanta@gmail.com*
[b] *Facultad de Ingenierías. Instituto Tecnológico Metropolitano. Medellín-Colombia. robinsonbuitrago@itm.edu.co*

Received: March 12th, 2020. Received in revised form: June 5th, 2020. Accepted: June 23th, 2020.

Abstract
Abrasive wear is an important problem in industrial applications. The wear of tools in the mining industry is a costly issue, and it reduces equipment uptime. This study examined welded coatings obtained using a manual metal arc process with improved wear resistance. Their microstructure was studied by optical and electron microscopy. ASTM G99 (pin-on-disc) and ASTM G65 (dry sand/rubber wheel) wear tests were performed, and the worn surfaces were inspected to understand the wear mechanisms. The results show that the coating has a hypereutectic microstructure composed of austenite, NbC, and M_7C_3 carbides. The size of the nanocarbides was 91 nm; and the volume content, 5.3%. Hardness values were found around 1029 $HV_{200\ g,\ 15\ seg}$. Low values of mass losses were attributed to the hypereutectic nanostructured hardfacing coating with extremely high hardness. The main wear mechanisms were microfracture and detachment of carbides and microcutting on the matrix.

Keywords: nanostructured; hardfacing; abrasion; hypereutectic.

Resistencia al desgaste y dureza de recubrimientos por soldadura nanoestructurados

Resumen
El desgaste abrasivo es un problema importante en aplicaciones industriales. El desgaste de las herramientas en la industria minera es un problema costoso y reduce el tiempo de funcionamiento de los equipos. En este trabajo se evaluaron recubrimientos soldados de alta resistencia al desgaste obtenidos mediante un proceso manual de arco metálico. La microestructura fue analizada por medio de microscopía óptica y electrónica. Se realizaron pruebas de desgaste ASTM G99 (pin-on-disc) y ASTM G65 (arena seca / rueda de goma), y se inspeccionaron las superficies desgastadas para comprender los mecanismos de desgaste. Los resultados muestran que el recubrimiento tiene una microestructura hipereutéctica compuesta de carburos de austenita del tipo NbC y M_7C_3. El tamaño de los nanocarburos fue de 91 nm; y el contenido del volumen, 5.3%. Los valores de dureza se encontraron alrededor de 1029 $HV_{200\ g,\ 15\ seg.}$. Se observaron bajas pérdidas de masa en el recubrimiento generadas por la microestructura hipereutéctica. Los principales mecanismos de desgaste fueron la microfractura y desprendimiento de carburos y microcorte en la matriz.

Palabras clave: nanoestructurados; recubrimientos duros; abrasión, hipereutécticos.

1. Introduction

The components of machinery used for processing cement or sugar cane, mining, earth moving, and rock and minerals handling can fail because of abrasive wear. Typically, the materials used for those applications have been superficially modified to control wear, but the cost of abrasion could reach 4% of the gross national product in industrialized countries [1].

Currently, numerous techniques for the deposition of hardened layers are available. Plasma spraying, laser cladding, hardfacing, thermal spraying, and chemical and physical vapor deposition are widely used to modify the surfaces. However, welding processes such as GMAW, SMAW, GTAW, and FCAW have emerged as solutions to improve wear resistance in metal-to-earth abrasive applications [2]. Among such metal manual arc processes, SMAW offers several advantages related to equipment cost

How to cite: Paz-Triviño, F, Buitrago-Sierra, R, and Santa-Marín, J.F, Wear resistance and hardness of nanostructured hardfacing coatings. DYNA, 87(214), pp. 146-154, July-September, 2020.

© The author; licensee Universidad Nacional de Colombia.

and the availability of filler materials, while GMAW and FCAW have a high deposition rate [3]. In turn, GTAW is very clean and produces no slag [4]. However, SMAW is preferred in the field since the equipment is portable and inexpensive. In addition, by using SMAW, carbides, which offer a high hardness, can be deposited and the matrix can be also tough [5].

Tungsten-based carbides have been traditionally used for hardfacing applications. Nevertheless, high-chromium alloys are also suitable for metal-to-earth applications since the hardness of M_7C_3 carbides can reach up to 1600 HV [6]. New alloys modified with other elements to promote carbide formation have been used to improve hardfacing properties. Some authors have studied FeCrC and FeCB [5] hardfacing alloys, new materials modified with tungsten carbides [7], and, recently, alloys with high Mo contents [8] and silicide-strengthened hardfacing steels [9].

Another way to improve wear resistance in alloys is to add niobium, molybdenum, and titanium to the Fe-C-B systems. Those elements are used to precipitate the hard phases [10]. Carbides are typically the hard phases; they appear in a blocky shape and in a volume content of approximately 5%, with hardness values between 1200 and $1900HV_{0.1kg}$ [11].

In recent years, nanostructured materials (NMs) and several consumables that deposit hard nanostructured coatings have been studied, focusing on their microstructural evolution and wear resistance. Tubular FCAW filler metals have exhibited outstanding properties due to their characteristics in the nanoscale compared to those of conventional grain materials [12]. Specifically, these materials show an extremely high hardness that could be explained by their small crystallite size, which ranges between 30 and 50 nm. They can also form ultrahard niobium precipitates and boron rich or with tungsten carbides which increase wear resistance [13].

In order to improve the wear resistance of hardfacing alloys, nanostructured rare earth oxides (REOs) have also been studied [11]. Wang et al. [11] analyzed the microstructure of nanostructured additives with rare earth oxides added to a high chromium cast iron (HCCI). They also characterized the primary carbide fraction volume and concluded that the use of nanostructured REOs increases the primary carbide fraction. Their study also included a pin-on-disk sliding wear experiment. Pin-on-disk tests have been used to explore the effect of nano-additives on wear rates [12]. Other authors have also investigated the effect of nano-additives on the wear rates measured by pin-on-disc tests [14]. In their case, when nano-additives were added to the alloy, the eutectic matrix seemed to support brittle carbides and avoid cracking in the coating. They also found that the K_{IC} of the coatings was improved by the presence of the additives, and, consequently, their wear resistance can also be improved by reducing microcracking.

In summary, hardfacing coatings deposited by SMAW can be used to quickly repair worn components in the mining industry. To the best of our knowledge, the literature includes a limited number of studies into the wear resistance of alloys containing Nb nanocarbides [15,13,16]; however, the available articles do not analyze nanocarbides in a coating made using a single layer. Therefore, the aim of this study is to evaluate the wear resistance of a single-layer nanostructured hardfacing coating deposited by SMAW. The outstanding hardness of the coating (around 71 HRc for a single layer) is considered one of its main characteristics. The coating is characterized as nanostructured by the manufacturer, and this study evaluates its properties (such as hardness, microstructure, and wear resistance) by two different laboratory tests. The main contribution of this article is the complete characterization of the microstructure of nanostructured coatings (including nanocarbides) and the evaluation of wear resistance of a single-layer coating.

2. Materials and methods

2.1. Materials and welding procedures

The nanostructured hardfacing coating was manually deposited by the shielded metal arc welding (SMAW) process. The coatings were manually applied, and a direct current electrode positive (DCEP) with a Millar Dynasty 35 power source was employed. The diameter of the hardfacing filler metal was 3.96 mm. An ASTM A36 steel test coupon (150x150x12.5 mm) was used to deposit the weld beads according to the ASME's IX Boiler and Vessel Pressure components code [17]. The chemical composition of the substrate provided by the manufacturer is detailed in Table 1.

Four ASTM A36 carbon plates (100x100x100 mm) were used to produce the weld beads and measure the dilution percentage. According to Dupont et al. [18], dilution is important for hardfacing coatings since it can significantly modify the coatings' chemical composition and, consequently, their microstructure. The test coupons were carefully cleaned using acetone and a power wire brush before welding. The electrodes were placed in an electric oven for two hours at 120 ºC. Two single weld beads were deposited on each test coupon using 135A and 150A (amperage values recommended by the manufacturer) at a constant travel speed of 7 in/min. No preheat/postweld heat treatment was applied. The total number of specimens for the dilution test was 8 (2 specimens per plate).

After welding, an abrasive cut wheel was used to remove two specimens from each test coupon. Every cross section was prepared by conventional grinding and using abrasive papers of 60, 120, 280, 400, 600, and 1000 grits to polish the specimens. The polished specimens were etched in a 2 wt pct Nital solution (see Fig. 1b). The samples were inspected in an optical microscope, and the free software ImageJ was used to measure the size and amount of carbides. The dilution was calculated by the equation proposed by Dupont et al. [18].

Table 1.
Nominal chemical composition of ASTM A36 steel.
IX (2015).

%C	%Si	%S	%Cu	%P	%Fe
0.25	0.40	0.05	0.20	0.04	Balance

Source: The Authors.

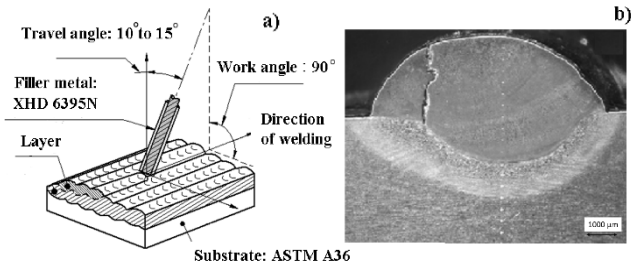


Figure 1. a) Scheme of the welding technique. b) Cross section used to measure dilution.
Source: The Authors.

Fig. 2 shows a longitudinal section of the final test coupon used to extract samples for the abrasion test and welded using a welding procedure specification (WPS) according to ASME's Boiler and Pressure Vessel Code [17], as summarized in Table 2. The WPS suggested the application of one hardfacing layer in the flat position (bead on plate) using the SMAW process without any preheat/postweld heat treatment. Additionally, applying the backhand welding technique, stringer overlapped beads were deposited without any transverse oscillation of the electrode (Fig. 1a). The single-layer deposit was placed along the full length of the plate using 135 amperes. The electrical welding parameters were kept constant, and the diameter of the electrodes was 3.97 mm (5/32"). The test coupon was left to cool down naturally to room temperature and a visual examination was performed to determine its acceptability according to the proposed WPS.

Liquid penetrant testing was used considering the minimum requirements in Table T-621 as the reference values [19].Type II (Visible Penetrant Examination) and Method C (Solvent Removable) were chosen based on Table 1 (Classification of Penetrant Examination Types and Method) and in agreement with SE-165 of Article 24. A universal grinder machine and a grinding wheel were used to grind both the hardfacing and the top surface (205x19x31.75 mm in size) at a maximum angular speed of 3600RPM (40m/s). The liquid penetrant method was employed to evaluate the material under the acceptance standards detailed in the procedure specification.

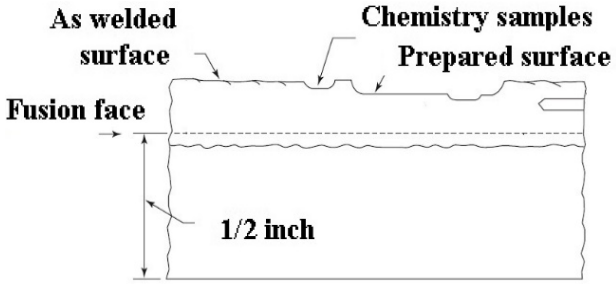


Figure 2. Scheme of longitudinal section of final test coupon.
Source: The Authors

Table 2.
Overview of Welding Procedure Specification (WPS). Essential variables in the special process (hard-facing overlay) according to ASME IX (2015).

Parameter	Value	Parameter	Value
Process	Manual SMAW	Technique	Forehand
Joints (QW-402)	t= 6mm	Type of Bead	String
Base Metal (QW-403)	P.No=1, Group=1, UNS Number SA-36	Electrical Characteristics (QW-409)	Number of layers: 1 Type of current and polarity; DCEP
Thickness	T< 12.7 mm	Current	125-150
Filler Metals (QW-404)	F-No=71, A-No= 6, Size= 3.97 mm (5/32 pulg), Rod,	Voltage	28-37
Hardness	67-70 HRC	Travel Speed	2.5-3.5 mm/seg
Position (QW-405)	Flat, bead-on-plate	Note	Cracks are allowed in the weld deposit
Interpass Temperature	T=120 °C	Chemical Composition	As reported in Table 1

Source: The Authors.

2.2. Hardness measurements

The hardness of the specimens was measured by the Vickers hardness test applying of a force of 2 kgf for 9s. The hardness of the hard phases was measured by the microhardness test, with a Vickers indenter, applying a force of 0.05 Kgf for 12s. The base metal, heat affected zone and the weld cross-sections central axes of the weld cross sections were indented every 500 µm.

2.3. Microstructure and chemical analysis

A set of 20x20-mm samples was used for microstructural characterization. They were metallographically polished and etched in a solution of Nital 2 % wt. A Nikon Eclipse Ci-L/S Light Optical Microscope (LOM) was used to analyze the microstructure and the carbides. The chemical composition was studied by Field-Emission Scanning Electron Microscopy (FE-SEM) in a JEOL JSM7100F and a backscattered electron detector (BED) in compositional mode. Furthermore, Energy Dispersive spectroscopy (EDS) was used for the elemental concentration. Image analysis was employed to determine the volume fraction of carbides.

X-ray diffraction characterization was performed to determine the carbides present in the hardfacing overlay. A Panalytical X'Pert Pro diffractometer with Cu-Kα radiation was employed with a step size of 0.002º from 15 to 140 2 tetha degrees and a time step of 9s. Optical emission

spectrometry (OES) and X-ray fluorescence spectrometry analysis were used for the chemical analysis.

2.4. Abrasive wear tests

ASTM G99 and ASTM G65 wear tests have been extensively used to measure wear resistance of hardfacing coatings. Previous studies [13] have reported a correlation between the number of layers and wear resistance measured according to ASTM G65-04. Other researchers have also used ASTM G99 to measure the wear resistance of hardfacing coatings, as demonstrated by Gualco et al. [16]. In their paper, two wear tests (ASTM G65 and ASTM G99) were performed.

In this study, the ASTM G99 test method was used for wear testing with a pin-on-disk apparatus. Water jet cutting was used for the extraction of the pins from the prepared test coupon once the top surface of the hardfacing was grinded using a universal grinder machine. Acetone was used to clean the surfaces of all the samples. All the samples were weighed in an electronic balance (Sartorius, +/- 0.01 mg). Flat-ended pins were employed during the tests. An abrasive cloth composed of alumina was used with abrasives 0.4 mm in size; their morphology is detailed in Fig. 3b.

The statistical software Minitab (free version) was used to analyze the variables (load and sliding speed), effects, and interactions in the tribotest using a factorial design. As the abrasive tests were not conducted on the same day, two blocks of experiments were proposed. Two levels of force, high and low, were defined at 20 N and 40 N, respectively, and the two levels of velocity were 0.4 m/s and 0.6 m/s. The predetermined level of significance was $\alpha = 0.05$ [20]. The ASTM G65 test (dry sand/rubber wheel abrasion test) was also performed to evaluate the wear behavior of the hardfacing coating. The wear tests were conducted using AFS 50/70 sand, whose morphology is shown in Fig. 3a. The test specimens were cut in rectangular shapes of 25x76 mm and between 3.2 and 12.7 mm thick. The sand was placed into a hopper and introduced between the specimen and the rotating wheel. Next, the specimen was pressed with 130 N by means of a lever while a constant rate of sand flow between 300 and 400 g/min was fed. As per ASTM G65, the duration of this abrasion test was 30 min. Before testing, acetone was used for cleaning the specimens, which were then weighted. Three tests were conducted at a room temperature of 24-27°C. Each test was run up to a sliding distance of (4309 m).

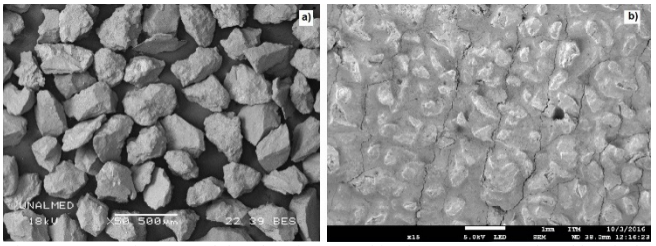


Figure 3. SEM images of the abrasives used in the tests: a) sand and b) cloth. Source: The Authors.

Generally speaking, both wear tests evaluate the abrasive resistance of coatings to abrasion. ASTM G65 can be considered as a three-body abrasion tests and ASTM G99 can be considered as a two-body abrasion test. Performing both tests will provide a complete outline of coating's resistance to abrasion

3. Results and discussion

3.1. Dilution measurements

Based on the results of the dilution measurements, the two amperage levels did not show a significant difference; however, the dilution obtained was consistent for shielding metal arc welding (20-45%) [21] (see Fig. 4). Welding current is not considered an essential variable and, consequently, any of the two amperages was appropriate to be used. However, to evaluate the proposed welding procedure and considering the dilution, 135 A was chosen as the most convenient amperage for the test. Since no significant variations in dilution were found with the two amperages, the microstructure of hardfacing alloy was expected to remain unmodified. The flat position (Bead On Plate, BOP) was used during the welding test by employing stringer beads and a backhand welding technique. Another important feature observed during the analysis of the cross section of the single pass welding is that there were cracks in the beads, as shown in Fig. 4b. Those cracks will be discussed in the next section. Fig. 4c shows some of the carbides in the microstructure, which will be discussed in detail in Section 3.3.

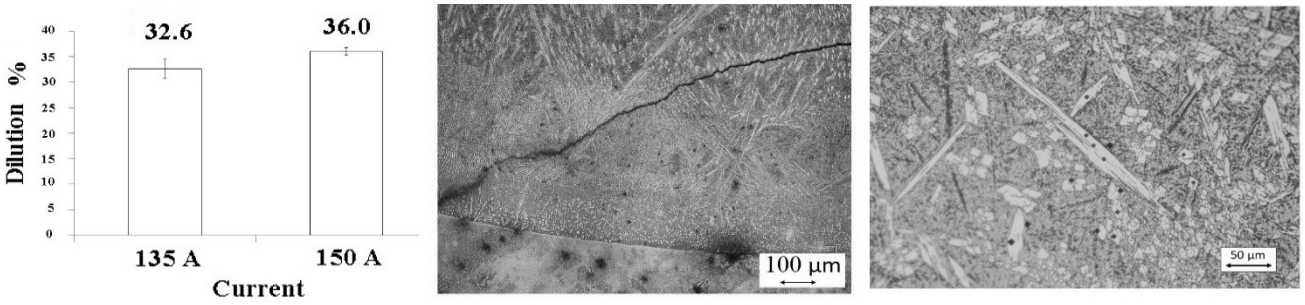


Figure 4. a) Dilution. b) Cross section of hardfacing cracks. c) Detail of carbides. Source: The Authors.

3.2. Visual inspection

The welding test coupon exhibited a good appearance and no spatter or undercut on the surface was identified (not shown). Transverse cracks were observed; they appeared once the first weld bead was deposited and then propagated to the neighboring bead.

Because these cracks were formed at high temperatures during the welding process, they are considered hot cracks. Such cracks were also characterized as weld solidification cracks, and they were formed by the natural shrinkage during the solidification process when the microstructure is susceptible [22] (see Fig. 4a). As suggested by the welding procedure specification, a liquid penetrant testing was performed, and the cracks were visible.

The cracks appeared because of differences in the thermal expansion between the deposited and the base metal. These differences generate strains in the hardfacing deposit created during the cooling. In addition, the chemical study of the hardfacing electrode revealed that it can be considered a high-alloy electrode; in the literature about applications without preheat treatments, these materials are susceptible to cracking and cross-checking [23]. Nevertheless, this discontinuity is not detrimental to hardfacing applications; in fact, cross checking can favor hardfacing applications by relieving stresses [1]. Cracks are allowed and they are not a major concern for the proposed WPS.

Table 3 shows the chemical analysis of the hardfacing deposit. When the results of the chemical composition (Cr and C contents) were plotted in a Jackson diagram [24] (not shown), the alloy was found to be hypereutectic, composed of primary carbides and a eutectic matrix, which is expected for this hardfacing alloy in the first layer. The high carbon and boron contents and the presence of carbide former Nb produce primary carbides even in the diluted first layer of the hardfacing deposit [25]. As the alloy is also rich in Cr and C, M7C3 carbides are created during the solidification due to segregation. M7C3 were chromium-rich while NbC are boron rich since they can be described as complex carbides where the B substitutes C in the lattice.

3.3. Microstructure and hardness

Fig. 5a shows the typical microstructure found on the hardfacing deposit surface. It has been reported that dilution is maximum next to the fusion line and, consequently, the microstructure is formed by austenite dendrites and secondary eutectic M7C3 carbides [26]. Fig. 5a shows the primary M_7C_3 (arrow 1), and arrow 2 in the same figure marks a zone with the eutectic microstructure. The microstructure of the ASTM A36 steel (not shown) is composed of ferrite and the hardness of the substrate is 160 ± 10 HV.

SEM/EDS analyses and their microhardness results confirm the nature of the carbides found in the hardfacing. Fig. 5b (arrow 1) shows elongated M_7C_3-type chromium carbides. These results are different from those obtained by J. Gou et al. [27], who found that carbides were arbitrarily oriented when the hardfacing was subjected to natural cooling conditions. Arrow 2 shows the carbides found in secondary dendritic arms. Arrow 3 in the same figure shows Nb-rich carbides dispersed all over the transverse section, and arrow 4 marks deformed Nb- and B-rich carbides. The manufacturer of this hardfacing coating welding electrode claims that the electrode was produced using nanotechnology [13]. The deposit can be characterized as nanostructured, with ultrahard niobium precipitates added to improve abrasion resistance. The hardness of some chromium carbides (in the microscale) was around 1000 HV. FE-SEM and BED (compositional images) were used to obtain images in the nanoscale, as shown in Fig. 5c. Such image shows

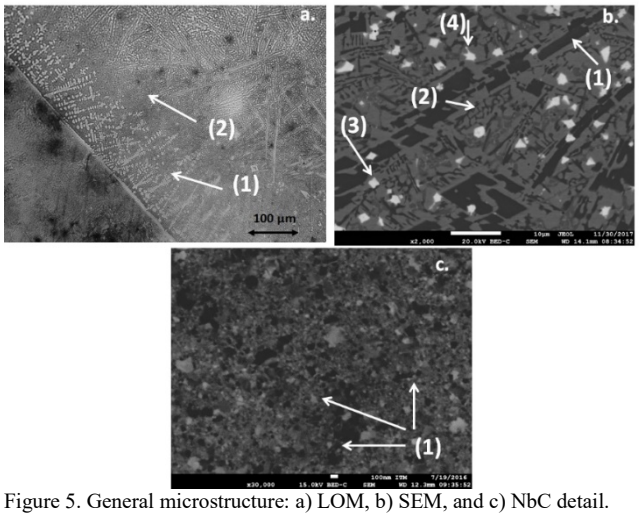


Figure 5. General microstructure: a) LOM, b) SEM, and c) NbC detail. Source: The Authors.

Table 3.
Chemical composition of hardfacing (one layer) and hardness values.

	%C	%Nb	%Cr	%B	%Fe	%Mn	%Si	Hardness
One layer (Measured by XRF)	3.8	3.4	13.2	1.3	81.2	0.3	0.42	1092±23.6
Phase 1 - Chromium carbide (Measured by EDS)	17.7	-	62.8	-	19.4	-	-	1592±73.8
Phase 2 - Niobium carbide (Measured by EDS)	21.7	71.2	2.4	-	4.5	-	-	Not measured
Phase 3 - Boron carbide (Measured by EDS)	22.7	54.2	2.3	17.4	3.2	-	-	Not measured

Note 1: All elements in weight %
Source: The Authors.

some nanostructured carbides with a mean size of approximately 91 nm, which implies that the alloy is effectively nanostructured according to the international standard ISO/TS 80004-1:2010 since the dimensions of the carbides are in the nanoscale. Said standard defines a nanostructured material as "*a nanostructured material is that one having internal nanostructure or surface nanostructure*". Therefore, as confirmed in SEM images, the size of the carbides developed with the coating process was found to be in the nanoscale and, according to the ISO definition, the coating could be deemed nanostructured. The authors evaluated the microhardness using a profile, but it did not provide reliable information since the microhardness varies depending on the location of the indentation (matrix or carbides.

Fig. 6 presents an EDS map with the main phases. Fig. 6 clearly shows the Nb carbides and another important detail about those carbides: some of them are boron-rich (see the bottom right figure). Energy dispersive spectroscopy (EDS) was also used to identify the carbides produced during the solidification of the overlay weld pool. The localized spectra are shown in Table 3. Based on these results, the carbides present in the hardfacing microstructure are classified as M7C3 (Nb-rich) and (Cr-rich) carbides. Due to the presence of chromium, iron, carbon, and low amounts of alloying components (such as silicon, manganese, boron, molybdenum, niobium, and the M7C3 carbides) and based on previous reports [27], the hardfacing investigated in this study was classified as chromium carbide (CCOs).

The volume content of Nb-rich carbides was found to be 5.3% v/v, and their distribution was homogeneous. The Cr-rich carbides were observed at a volume content of 43.6% v/v. Self-shielded flux cored wires produced a similar result in terms of carbide volume fraction of primary carbides, which remained at around 43.2 % wt. Moreover, the authors found that the primary carbide volume fraction in the hardfacing deposit without nano REOs was 17.1%; in turn, the primary carbide volume fraction increases to 28.8 wt% when the nano REOs reach a maximum of 22.2% [28]. The resistance to abrasive wear is expected to increase when the volume of carbides is higher for alloys with traditional M_7C_3 carbides [29]. The effect is unknow for nanostructured carbides but a volume of 43.65% of carbides is considered beneficial for this application.

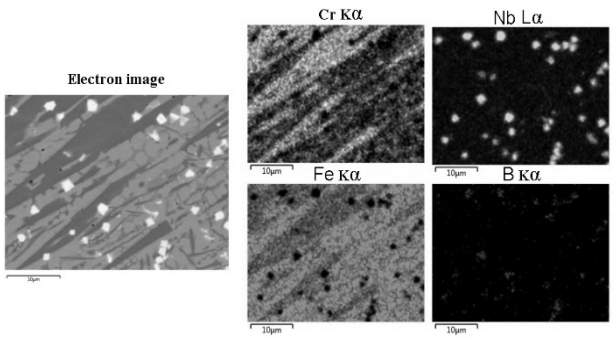


Figure 6. EDS map of different carbides.
Source: The Authors.

Fig. 7a presents the size distribution histograms of the Nb and Cr carbides, respectively. The Cr-rich carbides were found to be transversely oriented, with carbide clusters of 60 µm approximately. The distribution of the Cr-rich carbides longitudinally oriented is almost symmetric; their size ranges between 50µm and 100 µm, with some at 200 and 250 µm. Unlike, the histogram of Nb-rich carbides (see Fig. 7b) is nearly symmetric, with a mean size of carbides at around 2 µm. Those distributions did not take into account carbides with a mean size under 500 nm.

An additional test of a two-layer hardfacing application was performed using the same parameters described above, except for the current (150 A instead of 130 A). In terms of microstructure, the SEM images (not shown) exhibited a similar orientation and distribution of carbides compared to the single-layer application. In the two-layer application, primary Nb carbides were found in a volume fraction of 4.8%, whereas the Cr-rich carbides were found in a volume content of 40.2%. The variation in terms of microstructure was not substantial, even though the highest welding current was used for the two-layer application. These results are in agreement with those obtained by M. Kirchgaßner, E. Badisch, and F. Frane [11], who found Nb-rich carbides at a volume of 7% with a size of ≤ 3 µm in different shapes and Cr-rich carbides at a volume of 57.1 % with sizes between 30 and 200 µm. Although the volume fraction of small Nb-rich carbides is 5.3%, they can be considered the most important factor to increase abrasion resistance in the hardfacing deposit.

The XRD pattern of the hardfacing coating is presented in Fig. 7c. Austenite, NbC, and M_7C_3 can be identified, which is in agreement with the results published by other authors [15,30,31]. The microstructure can be found in the diagrams proposed by Jackson [24]. The micrographs (Fig. 5) confirm a hypereutectic microstructure. In this case, the microstructure is formed by primary carbides (proeutectic) inserted in the austenitic matrix.

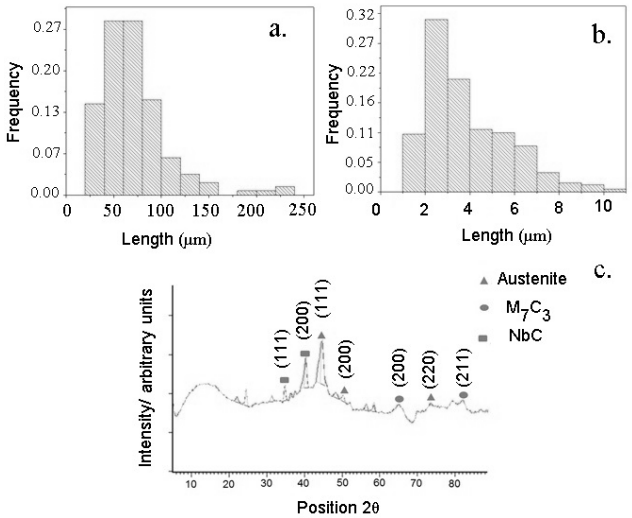


Figure 7. a) Histogram of chromium carbide. b) Histogram of NbC. c) X-ray pattern.
Source: The Authors.

The hardness of the coating and the hard phases is detailed in Table 3. The hardness of the coating (1029HV200 g, 15 s) is very similar to that of other nanostructured hardfacing coatings reported in the literature [12,13]. In the table, the microhardness of the primary carbides is 1592HV50 g, 15 seg. This value is also very similar to that reported in other studies into M_7C_3 carbides (1587HV50 g, 15 seg) [27,32]. Since the Nb-rich carbides were very small, it was not possible to perform hardness measurements.

3.4. Abrasive wear

Fig. 8 presents the mass losses of the coating after two different tests: ASTM G99 and ASTM G65. Fig. 8a details the values obtained after pin-on-disc tests. The base metal lost 1700 mg after the wear tests with high loads and a sliding distance of 204 m. The coating lost 37 mg at the same load and after running the tests for 2716 m. The wear rates of both materials were calculated; values of 8.3 mg/m in the base metal were obtained, in contrast with 0.013 mg/m in the nanostructured hardfacing coating. These values confirm a reduction of 638 times in terms of mass loss in the hardfacing coating compared to the base metal in the pin-on-disc test. An analysis of variance allowed us to conclude that the load effect is statistically significant at a p-value of 0.05 with a 95.22% confidence level. In addition, the interaction effect and sliding speed appear to be not significant when p-values higher than 0.05 are used.

A different behavior was found with low loads, and mass losses increased when the sliding speed was higher. This result probably indicates that a transition from a wear mechanism was found for the velocities under study. One plausible explanation found in the literature is that mass losses are higher since friction heating is expected to increase along with sliding speed [33]. However, a comprehensive understanding of this result is beyond the scope of this article.

Fig. 8b presents the mass losses after the dry-sand rubber wheel procedure (ASTM G65). The mass loss of the hardfacing was found to be 14 times lower than those obtained in the base metal. The difference between the results in the pin-on-disk tests and the dry-sand rubber tests can be explained by the fact that, in the first one, the pin passes over the same track repeatedly. Hence, lower mass losses are expected in pin-on-disk tests since the abrasive particles are detached from the cloth.

Fig. 9 shows the FE-SEM images of the worn samples, which present different wear mechanisms that can be identified. In Fig. 9a, arrows 1 and 2 show the microploughing on the surfaces due to abrasive wear; this is reflected in a deformed material on the side of the wear groove (see arrow 1 in Fig. 9a). Material removal by microcutting events can also be observed (arrow 2 in Fig. 9a). Fig. 9b is a back-scattering electron image where white regions represent the carbides, grey regions are associated with the matrix, and black regions mark the holes left by the spalled carbides. The wear track clearly appears as continuous parallel grooves indicated by arrow 1. The track can be observed as plastic deformation produced during abrasion. Moreover, the effect of carbides can also be seen in the same image. The carbides stop, to some extent, the continuity of the wear tracks that are generated (see arrow 2 in Fig. 9b) in the wear process. The same effect of Nb carbides was found in the overall wear performance previously reported by other authors [15].

Microcracking was also identified in the matrix at a higher magnification (see Fig. 9c). A brittle fracture is marked in the image with the arrows (2); this wear mechanism has been extensively reported in this kind of materials [14]. Finally, Fig. 9d presents carbides removal by spalling as well. In the figure, the arrows point to the holes left by the carbides, evidenced also by small residues of carbides left behind on the edges of the holes.

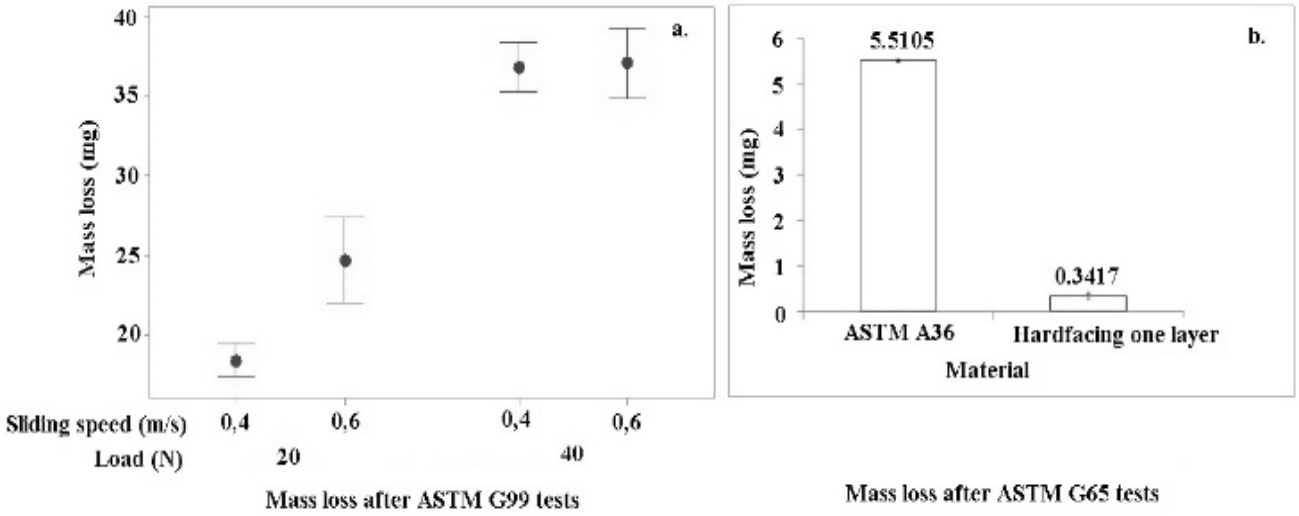


Figure 8. a) Mass losses after conducting ASTM G99 tests. b) Mass losses after conducting ASTM G65 tests.
Source: The Authors.

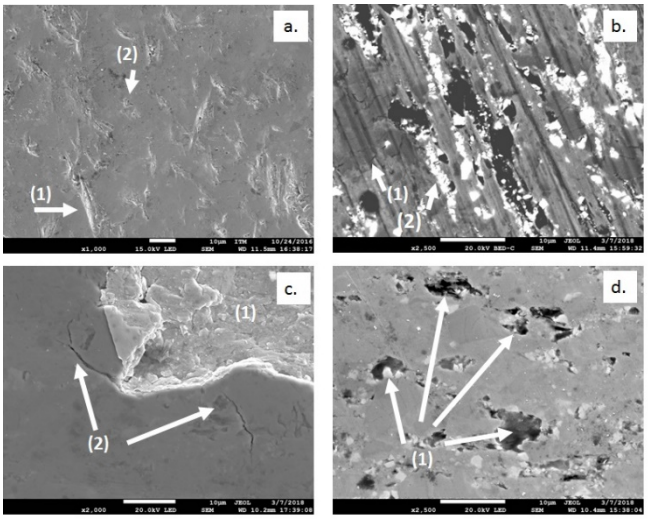


Figure 9. Wear mechanisms. a) Microcutting and microploughing on worn surfaces. b) Cracks and spalling of Nb carbides. Microcracks. d) Spalling near chromium carbides.
Source: The Authors.

4. Conclusions

A single layer of a nanostructured hardfacing alloy was studied in this paper. The results show that there is no variation in dilution using the welding parameters described above. The dilution was around 36%, and hardness values of 1029 HV 50 g, 15 seg were obtained in the weld metal overlay. The microstructure of the hardfacing coating was hypereutectic, and it was formed by an austenitic matrix with large (around 60 μm) proeutectic Cr-rich carbides (43.6%). There were also NbC (5.3%) in the microscale (around 2 μm) and other carbides (sizes under 91 nm) in the nanoscale.

Compared to the base metal (ASTM A36) used for the hardfacing, the wear resistance of the alloy was improved 14 times when tested in the dry-wheel rubber sand. When the hardfacing was tested in the pin-on-disc machine, the wear resistance did not change with different velocities if the load was high. When lower loads were used, the velocity had a significant effect on wear resistance. Microcracking, spalling of carbides, and microploughing were the predominant wear mechanisms identified in the SEM analysis of the pins worn surfaces.

Acknowledgments

The authors would like to thank the Welding Laboratory at Universidad Nacional de Colombia and the Polymeric Materials Laboratory and the Electron Microscopy Laboratory at Instituto Tecnológico Metropolitano.

References

[1] Lancaster, J.K., ASM handbook, vol. 18, friction, lubrication and wear technology, Tribology International, 26(4), pp. 293-294, 1993. DOI: 10.1016/0301-679X(93)90010-X
[2] Chaynes, P. and Farmer, H.N., Friction and wear behavior of hardfacing alloys, ASM Handbook., 18, 1992, 758 P.
[3] Armao, F., Byall, L., Kotecki, D. and Miller, D., Gas metal arc welding: product and procedure selection, Cleval. Lincoln Global. Inc, 2014.
[4] Khan, M.I., Welding science and technology. New Age International, 2007.
[5] Balasubramanian, V., Varahamoorthy, R., Ramachandran, C. and Muralidharan, C., Selection of welding process for hardfacing on carbon steels based on quantitative and qualitative factors., International Journal of Advanced Manufacture Technology., 40(9/10), pp. 887-897. 2009. DOI: 10.1007/s00170-008-1406-8
[6] Fan, C., Chen, M.C., Chang, C.M. and Wu, W., Microstructure change caused by (Cr,Fe)23C6 carbides in high chromium Fe-Cr-C hardfacing alloys, Surface and Coatings Technology., 201(3-4), pp. 908-912, 2006. DOI: 10.1016/j.surfcoat.2006.01.010
[7] Buchely, M.F., Gutierrez, J.C., León, L.M. and Toro, A., The effect of microstructure on abrasive wear of hardfacing alloys, in Wear, 259(1-6), pp. 52-61, 2005, DOI: 10.1016/j.wear.2005.03.002
[8] Dilawary, S.A.A., Motallebzadeh, A., Atar, E. and Cimenoglu, H., Influence of Mo on the high temperature wear performance of NiCrBSi hardfacings, Tribology International., 127, pp. 288-295, 2018. DOI: 10.1016/j.triboint.2018.06.022
[9] Bowden, D., Stewart, D. and Preuss, M., Understanding the microstructural evolution of silicide-strengthened hardfacing steels, Materials and Design, 161, pp. 1-13, 2019. DOI: 10.1016/j.matdes.2018.09.015
[10] Yüksel, N. and Şahin, S., Wear behavior-hardness-microstructure relation of Fe-Cr-C and Fe-Cr-C-B based hardfacing alloys, Materials and Design., 58, pp. 491-498, 2014. DOI: 10.1016/j.matdes.2014.02.032
[11] Kirchgaßner, M., Badisch, E. and Franek, F., Behaviour of iron-based hardfacing alloys under abrasion and impact, Wear, 265(5-6), pp. 772-779, 2008. DOI: 10.1016/j.wear.2008.01.004
[12] Gualco, A., Svoboda, H.G. and Surian, E.S., Study of abrasive wear resistance of Fe-based nanostructured hardfacing, Wear, 2016. DOI: 10.1016/j.wear.2016.04.011
[13] Gualco, A., Marini, C., Svoboda, H. and Surian, E., Wear resistance of Fe-based nanostructured hardfacing, Procedia Materials Science., 8, pp. 934-943, 2015. DOI: 10.1016/j.mspro.2015.04.154
[14] Gou, J., Lu, P., Wang, Y., Liu, S. and Zou, Z., Effect of nano-additives on microstructure, mechanical properties and wear behaviour of Fe-Cr-B hardfacing alloy, Applied Surface Science., 2016. DOI: 10.1016/j.apsusc.2015.11.076
[15] Correa, E.O., Alcântara, N.G., Valeriano, L.C., Barbedo, N.D. and Chaves, R.R., The effect of microstructure on abrasive wear of a Fe-Cr-C-Nb hardfacing alloy deposited by the open arc welding process, Surface Coatings and Technology., 276, pp. 479-484, 2015. DOI:

10.1016/j.surfcoat.2015.06.026
[16] Gualco, A., Svoboda, H.G., Surian, E.S. and de Vedia, L.A., Effect of welding procedure on wear behaviour of a modified martensitic tool steel hardfacing deposit, Materials Design., 31(9), pp. 4165-4173, 2010. DOI: 10.1016/j.matdes.2010.04.026
[17] Welding, B.S.P., Qualify processes and operators according to {ASME} Boiler and Pressure Vessel Code: Section {IX}, Welding Brazing Qualifications., 1, pp. 0-2, 2012.
[18] Dupont, J.N. and Marder, A.R., Thermal efficiency of arc welding processes, Weld. J., (December), pp. 406s-416s, 1995.
[19] ASME. Boiler and pressure vessel code, section V: nondestructive examination. American Society of Mechanical Engineers, 2004.
[20] Melvin-T., A., Reviewed Work: Applied statistics and probability for engineers by Douglas, C. and Montgomery, G.R. , Technometrics, 37(4), pp. 455-457, 1995. DOI: 10.2307/1269738.
[21] Pradeep, G.R.C., Ramesh, A. and Prasad, B.D., Hardfacing of AISI 1020 steel by arc welding in comparison with TIG welding processes., Journal of Science Resources., 5(1), pp. 119-126, 2013. DOI: 10.3329/jsr.v5i1.11899
[22] Lippold, J.C., Welding metallurgy and weldability. Wiley Blackwell, New Jersey, USA, 2014. DOI: 3390/met10010143
[23] T. Materials, ASM - Welding brazing and soldering, Engineering, 6, 1993, 2873 P.
[24] De Sairre-Balsamo, P.S., Scotti, A. and De Mello, J.D.B., Interpretation of hardfacing microstructure using Fe-Cr-C liquidus surface, Revista de Soldadura, 1995.
[25] Kotecki, J.D. and Ogborn, J.S., Abrasion resistance of iron-based hardfacing alloys, Welding Journal., 74(8), pp. S269-S278, 1995.
[26] Atamert, S. and Bhadeshia, H.K.D.H., Microstructure and stability of Fe□Cr□C hardfacing alloys, Materials Science and Engineering: A, 130(1). pp. 101-111, 1990.
[27] Mendez, P.F. et al., Welding processes for wear resistant overlays, Journal of Manufacture and Processes., 16(1), pp. 4-25, 2014. DOI: 10.1016/j.jmapro.2013.06.011
[28] Gou, J., Wang, Y., Sun, Z. and Li, X., Study of work function and dry sliding wear behavior of Fe-based hardfacing alloys with and without nano rare earth oxides, Journal of Alloys Compounds, 713C, pp. 255-265, 2017. DOI: 10.1016/j.jallcom.2017.04.172
[29] Zum-Gahr, K.H., Microstructure and wear of materials, vol. 10. Elsevier, 1987.
[30] Olaseinde, O.A., Van Der Merwe, J. and Cornish, L., Characterization and corrosion behaviour of selected duplex stainless steels in acidic and acidic-chloride solution, Advanced Chemical Enginnering Science., 4(January), pp. 89-93, 2014. DOI: 10.4236/aces.2014.41012
[31] Quan, C. and He, Y., Properties of nanocrystalline Cr coatings prepared by cathode plasma electrolytic deposition from trivalent chromium electrolyte, Surface and Coatings Technology., 269(1), pp. 319-323, 2015. DOI: 10.1016/j.surfcoat.2015.02.001
[32] Doğan, Ö.N. and Hawk, J.A., Effect of carbide orientation on abrasion of high Cr white cast iron, Wear, 189(1-2), pp. 136-142, 1995. DOI: 10.1016/0043-1648(95)06682-9
[33] Rai, D. and Pathak, J.P., Influence of sliding velocity on wear behaviour of different microstructures of Ni-Cr-Mo-V steel, Indian Journal Enginnering Materials Science., 11(2), pp. 113-120, 2004. DOI: 10.1016/0043-1648(95)06682-9

F Paz-Triviño, is a BSc. in Mechanical Eng. in 2005, MSc. Eng in Materials and Process Engineering in 2008, all of them from the Universidad Nacional de Colombia. His research interests include: materials, welding and non-destructive tests. Tribology and Surfaces Group, Universidad Nacional de Colombia.
ORCID: 0000-0002-7694-5276.

J.F. Santa-Marín, is a BSc. in Mechanical Eng. in 2005, MSc. Eng in Materials and Process Engineering in 2008 and PhD. in Engineering with emphasis on science and technology of materials in 2013), all of them from the from Universidad Nacional de Colombia. Currently, is a researcher for Advanced Materials and Energy (MATyER) Research Group at Instituto Tecnológico Metropolitano, Medellpin, Colombia. His interests include materials in general with emphasis on wear, processing, and physical-chemical and mechanical characterization of materials. He is coauthor of more than 12 international publications in international journals such as Tribology International, Wear, and others. Current filiation: Tribology and Surfaces Group, Universidad Nacional de Colombia and Facultad de Ingenierías. Instituto Tecnológico Metropolitano, Medellín.
ORCID: 0000-0001-5781-672X.

R. Buitrago-Sierra, is BSc in Chemist in 2005, from the University of Antioquia. Colombia. Advanced studies Diploma. Dept. of Materials in the University of Alicante Spain and PhD in Materials Science in 2012, from the University of Alicante, Spain. Currently, is a researcher for Advanced Materials and Energy (MATyER) Research Group at Instituto Tecnológico Metropolitano, Medellín, Colombia. His interests include synthesis and physical-chemical characterization of materials, nanotechnology and catalysis. Is coauthor of more than 30 international publications in international journals. Current filiation: Facultad de Ingenierías. Instituto Tecnológico Metropolitano.
ORCID: 0000-0002-5995-4031.

REGIONAL ATLÁNTICO

EL CENTRO DE COMERCIO Y SERVICIOS

CERTIFICA

Que FRANKLIN ALEXANDER PAZ TRIVIÑO identificado(a) con Cedula de Ciudadania No 98704990 de Bello, realizó y aprobó el curso de INDUCCION A PROCESOS PEDAGOGICOS con una intensidad horaria de Cuarenta (40) y obtuvo una evaluación Apto (A) con una equivalencia de (4.5).

Equivalencia de Evaluaciones:

D: Reprobó
A: Aprobó

Se expide en Barranquilla. a los dieciocho (18) días del mes de junio de dos mil veinte (2020)

Firmado Digitalmente por



YIZY YELINE CORTES PADILLA
Subdirector (E) CENTRO DE COMERCIO Y SERVICIOS
REGIONAL ATLÁNTICO

SENA: Una Organización con Conocimiento

La autenticidad de este documento puede ser verificada en el registro electrónico que se encuentra en la página web http://certificados.sena.edu.co, bajo el número 9302002120829CC98704990E.

American Welding Society

Certified Welding Inspector (CWI) with API 1104 Codebook
Test Results Notification

SOLDADURAS WEST ARCO
LTDA - Bogota, Colombia

2019-04-10

Account #:609867

Franklin Alexander Paz Trivino

Circular 73A #39-58
Apartamento 201
Medellin Antioquia
CO

This is a report pertaining to your test performance. Unfortunately, your examination scores or experience do not qualify you for CWI certification as this time. CWI certification requires a passing score of 72% or greater on each part of the exam, with a minimum of 5 years of experience. However, you have achieved CAWI certification, which requires a passing score of 60% or greater on each part of the exam, with a minimum of 2 years of experience. IF your certificate level has not changed, the same credentials remain. Your scores are shown below:

CWI - Part B	63%

If your average for the three parts is 72% or greater, you may retest only on the part(s) failed. If the average is below 72%, a complete retest is required. Candidates are permitted to take up to (3) retests within (3) years of the original exam date. Applicants may take the first retest(s) of the failed segment(s) without additional training. Any additional retests (2nd or 3rd retests) shall require documented evidence of additional training – 16 hours for a 1-part or 2-part retest; 40 hours for 3-part retest.

The following page provides you with an itemized report on your test performance broken down by question category. This analysis can assist you to identify the areas where you need to focus your training for any retest(s).

CWI - Part B

Figure 1 - Candidate Performance by Examination Category

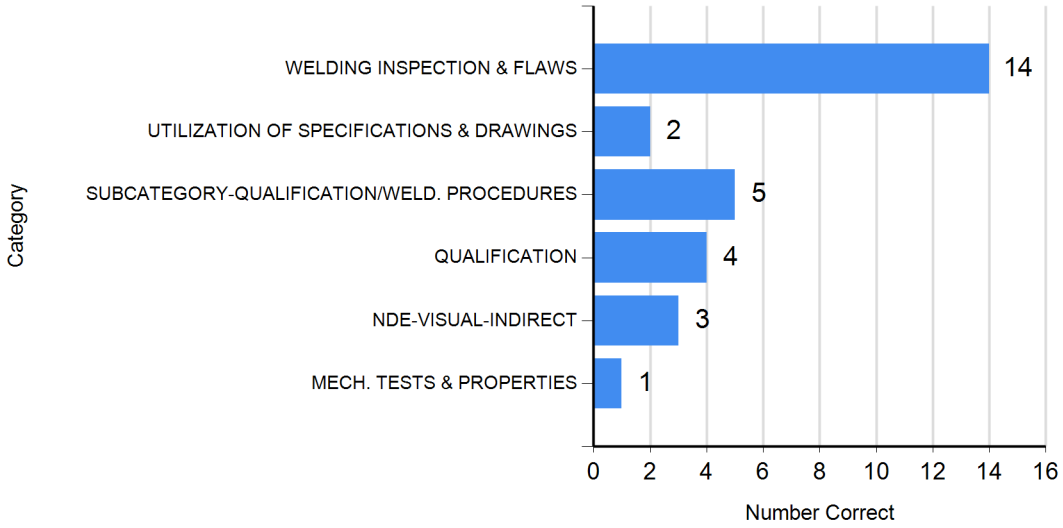


Figure 1 displays your performance by content category on the exam. Each blue bar indicates the number of questions you answered correctly in a content category. To find out the approximate total number of questions of each content category of the exam, please refer to the corresponding AWS Qualification and/or Certification document for each program which can be found on the AWS website.

This information is intended to give candidates an account of their relative strengths and weaknesses in content category performance. However, caution should be exercised when interpreting the information provided. First, some areas have very low number of questions. Caution is needed when interpreting performance based on small number of questions. Secondly, these scores cannot be used for recalculation purposes, as different weights are applied to the content categories when calculating the total score.